Pergamon

PII: S0277-5387(97)00172-1

Polyhedron Vol. 16, No. 23, pp. 4087–4095, 1997

0277-5387/97 $17.00+0.00

Preparation and structures of cobalt(III) complexes containing hydrotris(pyrazol-1-yl) borate and triamines

Akemi Hayashi,[a] Kiyohiko Nakajima[b] and Matsuo Nonoyama[a]*

[a]Department of Chemistry, Faculty of Science, Nagoya University, Chikusa, Nagoya 464-01

[b]Department of Chemistry, Aichi University of Education, Igaya, Kariya, Aichi 448, Japan

(Received 19 March 1997; accepted 21 April 1997)

Abstract—Cobalt(III) complexes of hydrotris(pyrazol-1-yl)borate (abbreviated as tp), $[Co(tp)_2]^+$ and $[Co(tp)(L)]^{2+}$ {L = diethylenetriamine (dien), N-(3-aminopropyl)ethylenediamine (pet), and 1,4,7-triazacyclononane (tacn)} were prepared and characterized spectroscopically. The ligand field spectra of the mixed ligand complexes deviated significantly from those anticipated by the average environmental rule. The structures of $[Co(tp)_2](PF_6)$, $[Co(tp)(tacn)](PF_6)_2$, and $[Co(tp)(dien)]Cl(PF_6)$ were determined by X-ray analysis. The Co—N bonds of $[Co(tp)_2]^+$ were short (average 1.927(3) Å) but the Co—N bonds of tp in $[Co(tp)(L)]^{2+}$ were unilaterally elongated (1.981(5) for L = tacn and 1.982(6) Å for L = dien) compared with the contracted Co—N bonds of tacn (1.941(5) Å) and dien (1.938(5) Å). These results would be cause of their ligand field spectral features. © 1997 Elsevier Science Ltd

Keywords: cobalt(III) complexes; hydrotris(pyrazol-1-yl)borate; 1,4,7-triazacyclononane; diethylenetriamine; N-(3-aminopropyl)ethylenediamine; X-ray structures.

Complexes of polypyrazolylborate anions exist in many metallic elements and form a large family of coordination and organometallic chemistry [1]. A hydrotris(pyrazol-1-yl)borate anion (abbreviated as tp) is one of the most extensively studied terdentate ligands and occupy a single face of a pseudo-octahedral or -tetrahedral metal complex. Coordination chemistry of octahedral cobalt(III) have, from a different viewpoint, been investigated extensively well [2] but cobalt(III) complexes coordinated with polypyrazolylborate anions are surprisingly scarce [1,3]. The complicated complex, $[Co(tp)_2][Sn_2Co_5Cl_2(CO)_{19}]$ obtained from the reaction of Ktp with $SnCl[Co(CO)_4]_3$, is a rare example of cobalt(III) complexes of tp [4]. In order to open up a new field in cobalt(III) complexes of polypyrazolylborate, we have, first of all, investigated cobalt(III) complexes coordinated with tp and terdentate amines L, Structure 1, {L = diethylenetriamine (abbreviated as dien), N-(3-aminopropyl)ethylenediamine (pet), and 1,4,7-triazacyclononane (tacn)}.

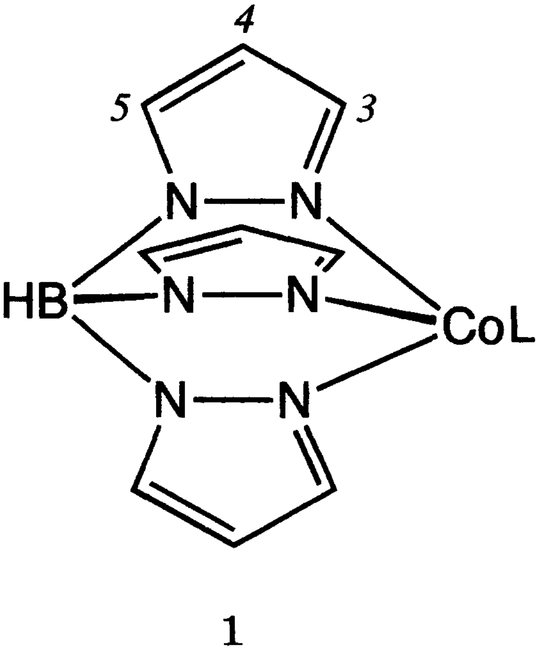

1

---

*Author to whom correspondence should be addressed.

RESULTS AND DISCUSSION

Hydrotris(pyrazol-1-yl)borate ion (tp) replaced all the ligands of $[CoCl(NH_3)_5]^{2+}$ to give $[Co(tp)_2]^+$ and the three Cl^- ligands of $[CoCl_3(L)]$ to afford $[Co(tp)(L)]^{2+}$ (L = tacn, dien, and pet). These complexes have been characterized spectroscopically (Tables 1 and 2), and the structures of $[Co(tp)_2]^+$ and $[Co(tp)(L)]^{2+}$ (L = tacn and dien) have been determined by X-ray analysis. The IR spectra of all the complexes show ν(B—H) bands at higher frequencies than those of the free ligand (2437 and 2404 cm^{-1}) and the cobalt(II) complex, $[Co(tp)_2]$ (2483 and 2460 cm^{-1}). The mixed ligand complexes have ν(N—H) bands near at 3300 cm^{-1} as expected. In the far infrared region, the spectrum of $[Co(tp)_2](PF_6)$ shows new bands at 421 and 459 cm^{-1} which are absent in that of Ktp and also in that of $[Co(tp)_2]$. The latter complex has a unique, broad strong band at 225 cm^{-1} which is also absent in the spectrum of Ktp. These new bands are assigned to ν(Co—N) bands and the higher frequency bands of $[Co(tp)_2](PF_6)$ suggest stronger Co—N bonds for Co^{III}, while weak Co—N bonds are inferred for Co^{II} from the low energy band. This fact has been confirmed by the X-ray analysis (*vide infra*). The more complicated spectra of the mixed ligand complexes are not readily assigned.

Formation of the desired complexes were undoubtedly confirmed by the ^1H and ^{13}C NMR spectra (in D_2O) (Table 1). In the spectra of $[Co(tp)_2]^+$ and $[Co(tp)(tacn)]^{2+}$, only one set of signals of tp are observed and all the pyrazolyl groups (abbreviated as pz) are equivalent [5]. For $[Co(tp)(dien)]^{2+}$, two sets of signals of tp are observed in a 1 : 2 intensity ratio and for $[Co(tp)(pet)]^{2+}$, three sets in a 1 : 1 : 1 intensity ratio, the former having a plane of symmetry while the latter being not symmetry. The chemical shift of H-3 of pz is significantly different between $[Co(tp)_2]^+$ and $[Co(tp)(L)]^{2+}$ (L = tacn, dien, and pet). In the former the proton is situated between two pz rings of another tp ligand but in the latter they are pointed toward aliphatic chelate rings or an open space. The H-3 of $[Co(pt)_2]^+$ may, therefore, be shielded by the aromatic ring current of pz. A related spectral feature has been reported for a similar d^6 complex, $[Ru(tp)_2]$ [5]; H-3 at 6.83d ppm (J = 1.4 Hz), H-4 at 6.13 (pseudo t), H-5 at 7.82d (2.5). The spectral patterns (^1H and ^{13}C) due to the amine ligands are also con-

Table 1. ^1H and $^{13}C\{^1H\}$ NMR spectra of tp and the complexes in D_2O (δ ppm against TMS and figures in parentheses are coupling constants, J, in Hz)

	Pyrazole ring protons[a]		
Compound	H-3	H-4	H-5
tp	7.66dd(1.8, 0.4)	6.32dd(1.8, 2.2)	7.39dd(2.2, 0.4)
$[Co(tp)_2]^+$	6.67d(2.2)	6.17t(2.3)	8.04d(2.5)
$[Co(tp)(tacn)]^{2+}$	7.99d(2.4)	6.42t(2.4)	7.80d(2.3)[b]
$[Co(tp)(dien)]^{2+}$	7.98d(2.4)*	6.37t(2.4)*	7.80d(2.3)*
	7.95d(2.4)	6.36t(2.3)	7.79d(2.2)[b]
(in dmso-d_6)[c]	8.09d(2.2)*	6.60t(2.4)*	8.30d(2.2)*
	8.61d(1.9)	6.59t(2.2)	8.25d(2.2)
$[Co(tp)(pet)]^{2+}$	8.13d(2.1)	6.42t(2.2)	8.00d(2.4)[b]
	7.80d(2.2)	6.37t(2.3)	7.98d(2.2)*
	7.66d(2.0)	6.34t(2.2)	

	Pyrazole ring carbons[a]			
Compound	C-3	C-4	C-5	Others[a]
tp	141.9	105.9	135.6	
$[Co(tp)_2]^+$	145.8	110.0	140.0	
$[Co(tp)(tacn)]^{2+}$	144.4	108.6	139.9	52.7
$[Co(tp)(dien)]^{2+}$	143.7*	108.3*	139.5*	56.6*, 43.7*
	143.3	108.8	139.0	
$[Co(tp)(pet)]^{2+}$	145.0	109.3	139.7	55.4, 48.3,
	143.1	108.4	139.4	45.1, 35.5,
	142.0	107.8	139.0	22.0

[a] The signals indicated by * have double intensity relative to the others.

[b] The signal due to H(B) was not identified. The CH_2 signals of tacn were observed at 3.14m and 3.72m, those of dien at 3.02m, 3.16m, 3.33m, and 3.89m, and those of pet at 2.22m (2H), 2.46m, 2.55m, 2.83m, 3.06m (2H), 3.24m, 3.33m, and 3.74m ppm.

[c] The CH_2 signals are at 2.91m, 3.05m, 3.31m, 3.86m, those of NH and NH_2 at 8.06, 6.40*, 5.88*, and that of H(B) at 4.61 ppm.

Table 2. Electronic spectra of aqueous solutions of Ktp and the complexes

Compound	Absorption maximum/10^3 cm^{-1} (log ε)[a]
tp	46.60(4.10)
$[Co(tp)_2]^+$	21.62(1.90), 27.0sh(2.5), 34.45(3.55), 46.0sh(4.5)
$[Co(tp)(dien)]^{2+}$	20.98(2.32), 27.0sh(2.5), 29.0sh(2.6), 38.0sh(3.6), 46.5sh(4.5)
$[Co(tp)(pet)]^{2+}$	20.49(2.23), 28.77(2.67), 38.0sh(3.8), 48.34(4.57)
$[Co(tp)(tacn)]^{2+}$	20.26(2.42), 26.5sh(2.3), 28.5sh(2.5), 38.0sh(3.7), 45.81(4.49)
$[Co(tacn)_2]^{3+}$	21.79(1.98), 30.03(1.94)[b]
$[Co(pet)_2]^{3+}$	20.79(1.97), 28.82(1.85)[b]
$[Co(tacn)(dien)]^{3+}$	21.65(1.89), 29.85(1.85)[b]
$[Co(tacn)(pet)]^{3+}$	21.28(2.03), 29.33(2.00)[b]
s-fac-$[Co(dien)_2]^{3+}$[d]	21.80(1.82), 30.00(1.89)[c]
u-fac-$[Co(dien)_2]^{3+}$[e]	21.50(1.97), 29.70(1.95)[c]

[a] sh = shoulder.
[b] Ref. [6].
[c] Ref. [7].
[d] s-fac = symmetrical facial.
[e] u-fac = unsymmetrical facial.

sistent with the symmetry of the complexes but no assignment of each signal is attempted so far. The signals of H(B) and H(N) were not detected in our experimental conditions (in D_2O). The ^1H chemical shifts of tp in the complexes shows appreciable solvent dependence: e.g. $[Co(tp)(dien)]^{2+}$ in dimethlsufoxide-d_6 (dmso-d_6) (Table 1), where a broad signal of H(B) is observable. The origin of the solvent dependence is difficult to be deduced and not studied further.

The electronic spectra of the complexes (in H_2O) are given in Table 2 together with some related data in the literature [6,7]. The first ligand field absorption bands ($^1T_1 \leftarrow {}^1A_1$) are observed in the typical region for a $[Co^{III}(N)_6]$ chromophore while the second bands ($^1T_2 \leftarrow {}^1A_1$) appear as shoulders. Intense absorptions ($3 > \log \varepsilon$) in the UV region are due to charge transfer transitions and absorptions within ligands. Detailed inspection of the spectra clarifies some features. Of $[Co(tp)_2]^+$, the chelate rings being all six-membered, the position of the first band is close to those of $[Co(tacn)_2]^{3+}$ and $[Co(dien)_2]^{3+}$, the chelate rings of the two complexes being all five-membered. The strong ligand field of tp in $[Co(tp)_2]^+$ should be originated from short Co—N bond lengths revealed by X-ray analysis (*vide infra*). It is noteworthy that two shoulders are observed for $[Co(tp)(tacn)]^{2+}$ in the second band region (Fig. 1) (two less distinct shoulders are similarly observed for $[Co(tp)(dien)]^{2+}$) but interpretation of the phenomenon is not found so far (the X-ray analysis suggests a distortion: Co—N bond lengths are clearly different between tp, and tacn and dien ligands).

The band positions of ligand field absorptions of mixed ligand cobalt(III) complexes are, in general, situated at the average position of those of parent homoleptic ligand complexes (the average environmental rule) [6]. Examples are given in Table 2 ($[Co(tacn)(dien)]^{3+}$ and $[Co(tacn)(pet)]^{3+}$). The positions of absorption maxima of the mixed ligand complexes prepared in this study deviate significantly from those anticipated from the general rule. The deviation is very marked for $[Co(tp)(tacn)]^{2+}$; the band is observed at 20.26×10^3 cm^{-1}, being anticipated at 21.70×10^3 cm^{-1}. This fact implies the weakening of ligand field in the mixed tp complex. The origin seems to be due to the lengthening of the Co—N bonds caused by interligand repulsion between tp and tacn. The deviation is reduced for $[Co(tp)(dien)]^{2+}$ and some relief of interligand repulsion is expected for this complex because dien is sterically milder, forming two five-membered chelate rings with more flexibility than tacn forming three five-membered ones with fixed conformation imposed by its cyclic structure. The enhanced intensity of the ligand field transitions (large

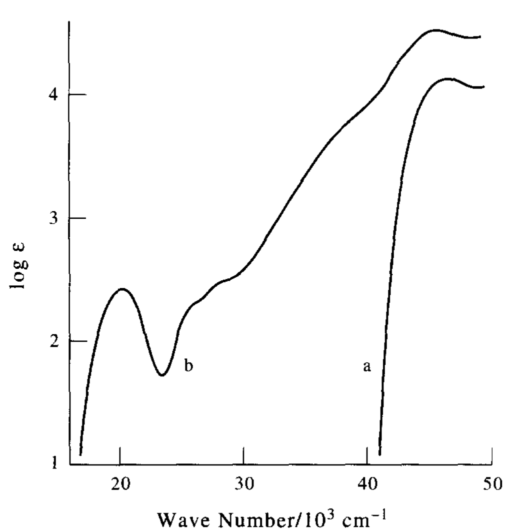

Fig. 1. Electronic spectra of (a) tp and (b) $[Co(tp)(tacn)](PF_6)_2$ in H_2O.

Table 3. Selected intramolecular distances (Å) and angles (°) of $[Co(tp)_2](PF_6)$ with e.s.d. in parentheses

Co(1)—N(11)	1.924(3)	Co(2)—N(21)	1.930(2)
Co(1)—N(12)	1.927(2)	Co(2)—N(22)	1.930(3)
Co(1)—N(13)	1.925(3)	Co(2)—N(23)	1.927(3)
N(11)—Co(1)—N(12)	89.7(1)	N(21)—Co(2)—N(22)	88.5(1)
N(11)—Co(1)—N(13)	88.6(1)	N(21)—Co(2)—N(23)	89.7(1)
N(11)—Co(1)—N(11′)	180[a]	N(21)—Co(2)—N(21′)	180[a]
N(11)—Co(1)—N(12′)	90.3(1)	N(21)—Co(2)—N(22′)	91.5(1)
N(11)—Co(1)—N(13′)	91.4(1)	N(21)—Co(2)—N(23′)	90.3(1)
N(12)—Co(1)—N(13)	89.4(1)	N(22)—Co(2)—N(23)	89.4(1)
N(12)—Co(1)—N(11′)	90.3(1)	N(22)—Co(2)—N(21′)	91.5(1)
N(12)—Co(1)—N(12′)	180[a]	N(22)—Co(2)—N(22′)	180[a]
N(12)—Co(1)—N(13′)	90.6(1)	N(22)—Co(2)—N(23′)	90.6(1)
N(13)—Co(1)—N(11′)	91.4(1)	N(23)—Co(2)—N(21′)	90.3(1)
N(13)—Co(1)—N(12′)	90.6(1)	N(23)—Co(2)—N(22′)	90.6(1)
N(13)—Co(1)—N(13′)	180[a]	N(23)—Co(2)—N(23′)	180[a]

[a] Strict 180° imposed by symmetry.

log ε values) should result from the distortion from a regular octahedral ligand field. This argument is checked by X-ray analysis of the mixed complexes (*vide infar*).

The unit cell of $[Co(tp)_2][PF_6]$ contains two independent molecules and the Co centers occupy the crystallographically special positions (x/a, t/b, z/c: 1, 0, 0 and 1/2, 1/2, 0). The two, only slightly distorted octahedral structures of $[Co(tp)_2]^+$ are very similar to each other and one of them is shown in Fig. 2 together with atom labeling. The selected bond distances and angles are given in Table 3. These data are fairly consistent with those previously reported for the complicated complex, $[Co(tp)_2][Sn_2Co_5Cl_2(CO)_{19}]$, where the Co—N bonds are slightly shorter with larger scattering (1.911(6), 1.918(6), 1.926(6) Å) [4]. The short Co—N bonds should be one of the origin of the strong ligand field of tp in $[Co(tp)_2]^+$. The bonds are far shorter than those reported for $[Co^{II}(tp)_2]$ (2.120–2.140(8) Å) [8]. The difference reflects clearly on ν(Co—N) frequencies. There is no interligand nonbonded H···H interaction in $[Co(tp)_2]^+$ because the H···H separations are well above the sum of the van der Waals radius of hydrogen (1.20 Å) (the closest H{C(14)}···H{C(11)} distance is calculated to be 3.04 Å).

Table 4. Selected intramolecular distances (Å) and angles (°) of $[Co(tp)(tacn)](PF_6)_2$ and $[Co(tp)(dien)]Cl(PF_6)$ with e.s.d. in parentheses

$[Co(tp)(tacn)](PF_6)_2$			
Co—N(1)	1.944(5)	Co—N(2)	1.933(6)
Co—N(3)	1.945(4)	Co—N(4)	1.989(5)
Co—N(6)	1.978(5)	Co—N(8)	1.977(5)
N(1)—Co—N(2)	86.2(2)	N(1)—Co—N(3)	84.8(2)
N(2)—Co—N(3)	84.8(2)	N(1)—Co—N(4)	176.7(2)
N(1)—Co—N(6)	89.0(2)	N(1)—Co—N(8)	95.3(2)
N(2)—Co—N(4)	90.5(2)	N(2)—Co—N(6)	94.7(2)
N(2)—Co—N(8)	175.8(2)	N(3)—Co—N(4)	95.7(2)
N(3)—Co—N(6)	173.8(2)	N(3)—Co—N(8)	91.5(2)
N(4)—Co—N(6)	90.5(2)	N(4)—Co—N(8)	88.0(2)
N(6)—Co—N(8)	89.2(2)		
$[Co(tp)(dien)]Cl(PF_6)$			
Co—N(1)	1.927(7)	Co—N(2)	1.943(4)
Co—N(3)	1.976(7)	Co—N(4)	1.985(5)
N(1)—Co—N(2)	87.0(2)	N(1)—Co—N(3)	174.5(2)
N(1)—Co—N(4)	96.0(2)	N(2)—Co—N(3)	89.1(2)
N(2)—Co—N(4)	176.5(2)	N(2)—Co—N(2′)	91.8(2)
N(2)—Co—N(4′)	90.0(2)	N(3)—Co—N(4)	87.9(2)
N(4)—Co—N(4′)	88.1(2)		

To resolve the ligand field spectral anomaly of the mixed ligand complexes, their structures have been studied. The structure of $[Co(tp)(tacn)]^{2+}$ is shown in Fig. 3 and the selected bond distances and angles are given in Table 4. The Co—N bond distances of tp (the average Co—N, 1.981(5) Å) are significantly elongated compared with those of $[Co(tp)_2]^+$ (1.927(3) Å). The Co—N distances of tacn (the mean value, 1.941(5) Å) are worth discussing if we consider the data in the literature. The corresponding bond distances in $[Co(tacn)(dien)]^{3+}$ are 1.966(7) Å (average) [6], those in $[Co((R)\text{-metacn})_2]^{3+}$ 1.974(5) Å ((R)-metacn = (R)-2-methyl-1,4,7-triazacyclononane) [9], and those in $[(tacn)Co(\mu\text{-}OH)_3Co(tacn)]^{3+}$ 1.932(4) Å (average) [10]. If there are no interligand and intraligand H···H nonbonded repulsion, a strain free Co^{III}—N length of most amine ligands has been estimated to be 1.925 Å and a stretch from the value reflects the repulsion [11]. In the dimer, therefore, the repulsion is very small as expected from the structure, while significant repulsion operates in the other two reported complexes. For $[Co(tp)(tacn)]^{2+}$, calculated interligand H···H distances are shorter than the sum

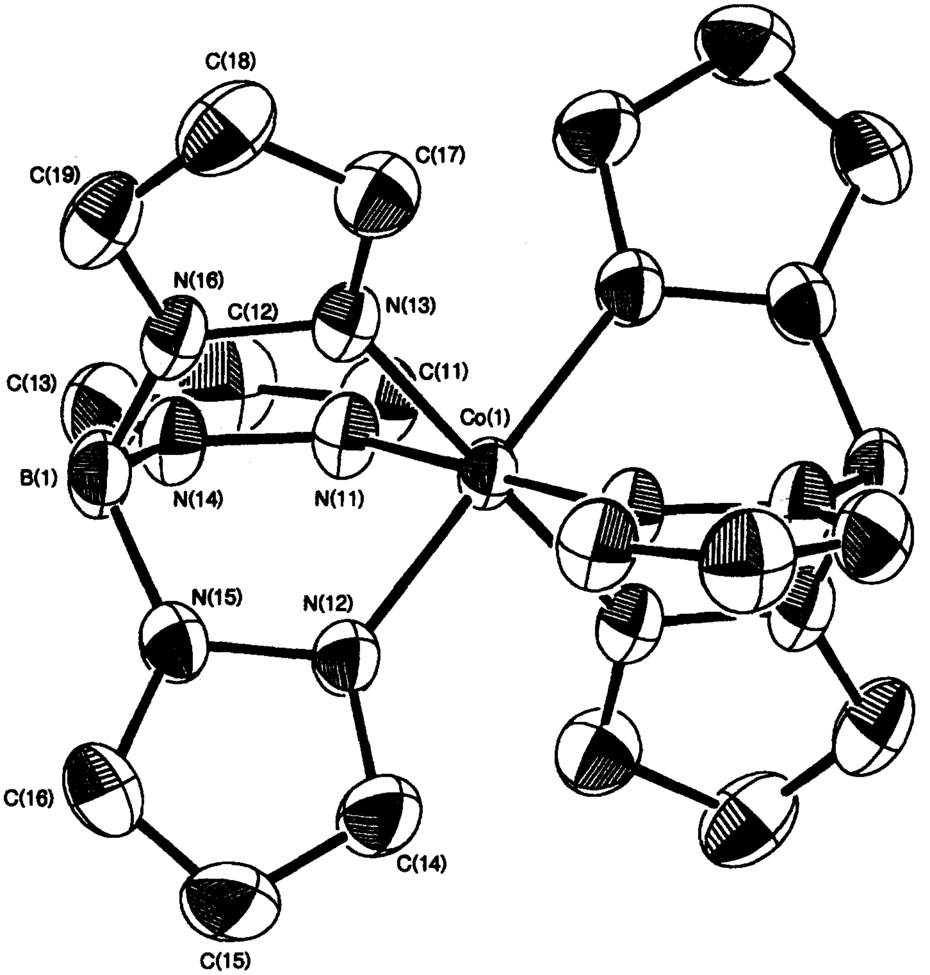

Fig. 2. ORTEP drawing and atom numbering scheme for one (x/a, y/b, z/c = 1, 0, 0) of the two independent molecules of $[Co(tp)_2](PF_6)$.

of the van der Waals radius of hydrogen: H{C(7)}· · ·H{C(4)}, 1.97 Å, H{C(10)}· · ·H{C(2)}, 2.00, and H{C(13)}· · ·H{C(6)}, 2.22, producing interligand strain. The Co—N bonds of tacn in $[Co(tp)(tacn)]^{2+}$ are slightly stretched (0.016 Å) by such repulsion (although shorter than those of $[Co(tacn)(dien)]^{3+}$ and $[Co((R)\text{-metacn})_2]^{3+}$), but those of tp far more (0.054 Å). The strain is, thus, mainly relaxed through unilateral stretching of the Co—N bonds of tp. The intraligand N—Co—N angles (average) are also different between the two ligands; 89.2° for tp and 85.3° for tacn. These facts seem to be caused by the dissimilarity in ligand properties of tp and tacn. The unilateral distortion of the coordination sphere may be one of the origin of the abnormality pointed above in the ligand field spectrum.

$[Co(tp)(dien)]^{2+}$ has a plane of symmetry as shown in Fig. 4 and its bond distances and angles are given in Table 4. The Co—N bond distances for dien (mean, 1.938(5) Å) is shorter than those reported [12,13] (1.96(1) Å for s-*fac*-$[Co(dien)_2]^{3+}$, 1.964(5) Å for u-*fac*-$[Co(dien)_2]^{3+}$, and 1.965(8) for $[Co(tacn)(dien)]^{3+}$) but the Co—N lengths for tp (mean, 1.982(6) Å) is much longer than those of $[Co(tp)_2]^+$ (mean, 1.927(3) Å). To relieve interligand overcrowding (between tp and dien) the tp ligand is unilaterally separated from the Co atom too much and hence the dien ligand will closely approach to the Co atom. This situation is very similar to the one discussed just above and would be reflected similarly on the ligand field spectrum. The calculated interligand H· · ·H distance between H{C(1)} and H{C(6′)} is 2.10 Å and that between H{C(3)} and H{N(2)} is 2.38 Å. The others are separated from each other more than 2.4 Å. Intraligand N—Co—N angles are rather similar between dien (average 88.6°) and tp (88.0°) in comparison with the difference between those of tacn and tp of $[Co(tp)(tacn)]^{2+}$. This should reflect the fact that acyclic dien is more flexible than cyclic tacn. The chelate rings of dien adopt a $\delta\lambda$-conformation while those of tacn are fixed to a $\lambda\lambda\lambda$- or a $\delta\delta\delta$-conformation. No crystals of $[Co(tp)(pet)]^{2+}$ suitable for X-ray analysis have unfortunately been obtained so far.

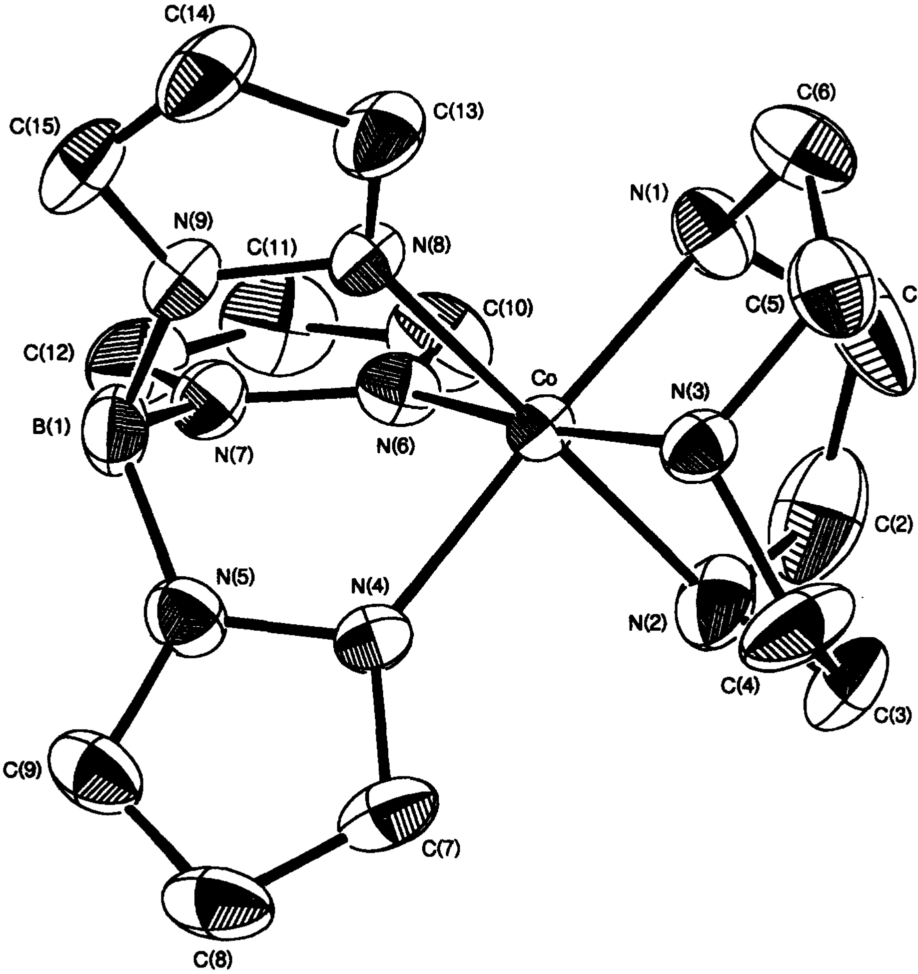

Fig. 3. ORTEP drawing and atom numbering scheme for $[Co(tp)(tacn)](PF_6)_2$.

EXPERIMENTAL

Measurements

NMR spectra (^1H and $^{13}C\{^1H\}$) were recorded on Hitachi R-90H and Bruker AMX-400 NMR spectrometers at ambient temperature and tetramethylsilane (TMS) was used as an internal standard. IR spectra were measured on a Perkin Elmer System 2000 FT IR spectrometer and UV–vis absorption spectra on Hitachi U-3410 and JASCO V-560 spectrophotometers. Elemental analysis was performed on a Leco CHN 900 analyser.

Preparation

Potassium hydrotris(pyrazol-1-yl)borate (Ktp), $CoCl_3(dien)$, $CoCl_3(pet)$, and $CoCl_3(tacn)$ were obtained by the literature methods [14,15,16]. $[Co(tp)_2]PF_6$: A mixture of 1 mmol (250 mg) of $CoCl(NH_3)_5$, 2 mmol (504 mg) of Ktp, and 80 mg of activated charcoal in 50 mL of water was stirred at 90°C overnight and filtered. Upon standing the filtrate gave a precipitate, $[Co(tp)_2]Cl \cdot 2H_2O$ (0.17 g, 31% yield), which was dissolved in 10 mL of methanol and mixed with an aqueous solution of 1.0 g of $NaPF_6$. The resulting precipitate was collected and recrystallized from acetone to give orange crystals in a yield of 11% (70 mg). M.p. >300°C (dec.). Calcd for $C_{18}H_{20}N_{12}B_2CoPF_6$: C, 34.3; H, 3.2; N 26.7%. Found: C, 34.5; H, 3.2; N, 26.6%. IR (Nujol): ν(B—H) 2518, 2530 cm^{-1}. $[Co(tp)_2]Cl \cdot 2H_2O$; Cacld for $C_{18}H_{24}N_{12}O_2B_2ClCo$: C, 38.9; H, 4.4; N, 30.2%. Found: C, 38.2, H, 4.2; N, 30.2%. IR: ν(B—H) 2548 cm^{-1}. This chloride is soluble in chloroform, dichloromethane, acetone, ethanol, methanol, nitromethane, and acetonitrile but insoluble in tetrahydrofuran and toluene. $[Co(tp)_2]^+$ can be used as a large cation to crystallize large anions.

$[Co(tp)(dien)]Cl_{1/2}(PF_6)_{3/2}$. A dimethylsulfoxide (dmso) solution (50 mL) of 2 mmol (537 mg) of $CoCl_3(dien)$ and 2 mmol (504 mg) of Ktp was stirred at 45°C for 10 min and poured in 100 mL of water. The solution was filtered and diluted with 5 L of water. The diluted solution was passed through an SP-

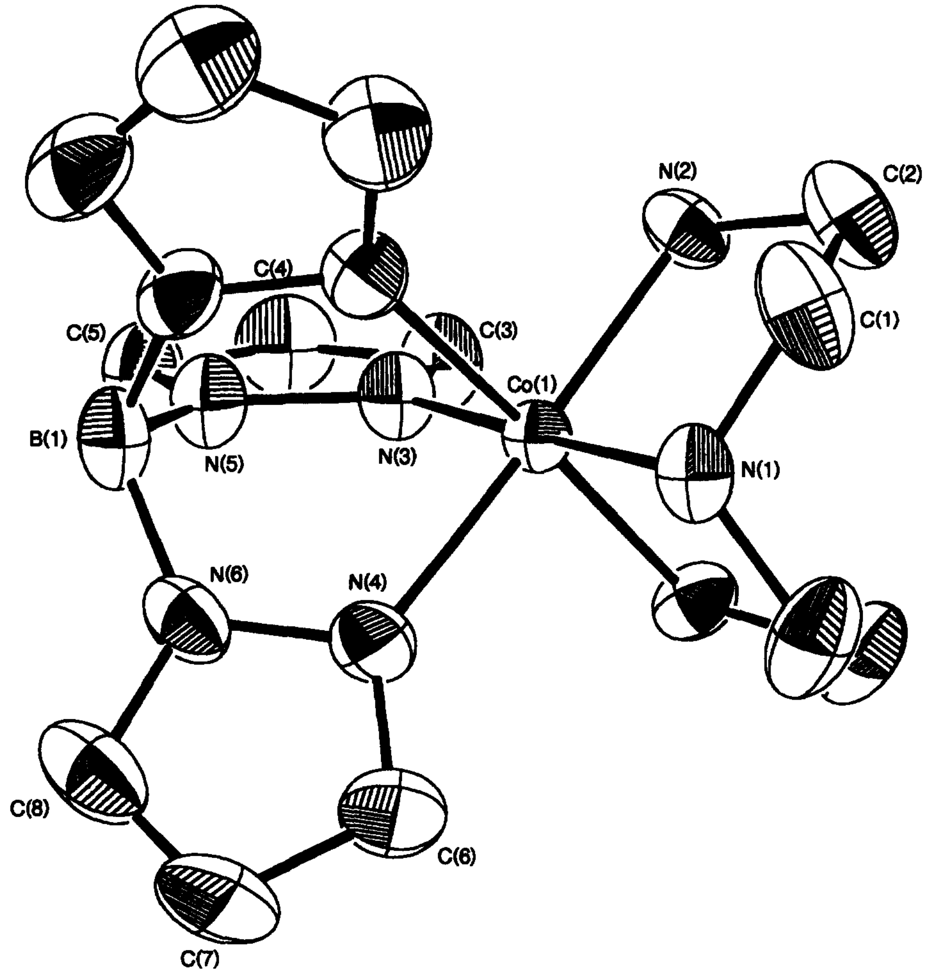

Fig. 4. ORTEP drawing and atom numbering scheme for [Co(tp)(dien)]Cl(PF_6).

Sephadex C-25 column (3ϕ × 20 cm) and the adsorbed band was eluted with 0.1 M of aqueous sodium chloride to develop three components: a small yellow band, a main orange band, and a small red band in the order of elution. The second orange band was eluted with 0.4 M aqueous sodium chloride and the collected effluent was evaporated to dryness under reduced pressure. The residue was extracted with 50 mL of methanol and on removal of the methanol the extract gave an orange solid, which was redissolved in 50 mL of methanol, filtered, and mixed with a methanol solution (6 mL) of 2.0 g of NH_4PF_6. Upon concentration of the solution to 30 mL and standing for a week orange crystals were obtained, which was recrystallized from acetone–ethanol (1/1) to give the product in a yield of 25% (330 mg). M.p. 246°C (dec). Calcd for $C_{13}H_{23}N_9BCoP_{3/2}F_9Cl_{1/2}$: C, 25.6; H, 3.8; N, 20.7%. Found: C, 25.7; H, 3.9; N, 20.7%. IR: ν(N—H), 3313; ν(B—H), 2509, 2521 cm^{-1}.

In a similar manner orange [Co(tp)(pet)](PF_6)$_2$ (reaction conditions; 35–40°C for 10 min and a second red band was collected) and pinkish orange [Co(tp)(tacn)](PF_6)$_2$ (70°C for 5 min and a third red band) were obtained.

[Co(tp)(pet)](PF_6)$_2$. M.p. 210–216°C. Calcd for $C_{14}H_{25}N_9BCoP_2F_{12}$: C 24.8; H, 3.7; N, 18.6%. Found: C, 24.6; H, 3.7; N, 18.5%. IR: ν(N—H), 3311, 3303; ν(B—H), 2507 cm^{-1}.

[Co(tp)(tacn)](PF_6)$_2$. M.p. 250°C (dec). Calcd. for $C_{15}H_{25}N_9BCoP_2F_{12}$: C, 26.1; H, 3.6; N, 18.2%. Found: C, 26.1; H, 3.7; N, 18.3%. IR: ν(N—H), 3292; ν(B—H), 2540 cm^{-1}.

X-ray analysis

Crystals of [Co(tp)$_2$](PF_6) suitable for X-ray analysis were obtained upon recrystallization from ethanol and slow evaporation of aqueous solutions of [Co(tp)(tacn)](PF_6)$_2$ and [Co(tp)(dien)]Cl$_{1/2}$(PF_6)$_{3/2}$ afforded suitable crystals (in the latter case, [Co(tp)(dien)]Cl(PF_6) crystallized). The crystallographic data and experimental details are given in Table 5. Data for each of the complexes were collected on a Rigaku AFC7R diffractometer with graphite-monochromatized Mo-Kα radiation. The unit cell parameters and the crystal orientation matrices were obtained by least-squares fit of 25 well-centered

Table 5. Crystallographic data and experimental details

Complex	$[Co(tp)_2](PF_6)$	$[Co(tp)(tacn)](PF_6)_2$	$[Co(tp)(dien)]Cl(PF_6)$
Formula	$C_{18}H_{20}N_{12}B_2CoF_6P$	$C_{15}H_{25}N_9BCoF_{12}P_2$	$C_{13}H_{23}N_9BClCoF_6P$
*F*w	629.96	691.03	555.55
Crystal system	triclinic	monoclinic	monoclinic
Space group	$P\bar{1}$ (No. 2)	$P2_1/c$ (No. 14)	*Cm* (No. 8)
a, Å	11.899(3)	9.052(2)	14.145(1)
b, Å	12.120(2)	16.418(2)	10.380(1)
c, Å	11.688(2)	17.328(2)	7.978(1)
α, °	113.04(2)		
β, °	113.05(2)	96.43(1)	107.13(1)
γ, °	100.06(2)		
Z	2	4	2
V, Å^3	1315.9(7)	2559.0(7)	1119.4(2)
μ(Mo-Kα), cm^{-1}	7.84	9.02	10.24
Transm factor	0.971–1.000	0.891–0.976	0.913–1.000
Crystal color	orange	orange	orange
Crystal habit	prismatic	prismatic	prismatic
Crystal size, mm^3	0.4 × 0.4 × 0.3	0.1 × 0.2 × 0.3	0.2 × 0.2 × 0.4
d_{calc} (g/cm^3)	1.59	1.79	1.65
λ(Mo-Kα), Å	0.71069	0.71069	0.71069
T, K	298	298	298
Scan range, °	$1.25+0.50\tan\theta$	$1.31+0.30\tan\theta$	$1.68+0.30\tan\theta$
Scan mode	ω-2θ	ω-2θ	ω-2θ
Scan speed, (°/min)	8	8	8
$2\theta_{max}$, °	60	60	60
No. of reflections measd	8036	6709	1779
No. of reflections obsd [$\|F_o\| > 3\sigma(\|F_o\|)$]	5251	3764	1699
R	0.047	0.064	0.047
R_w	0.051	0.077	0.062
s	1.66	2.73	3.25
$(\Delta/\delta)_{max}$	0.11	0.12	0.50
Largest diff peak (e/Å^3)	0.49	0.94	0.53
Largest diff hole (e/Å^3)	−0.70	−0.56	−0.88

$R = \Sigma||F_o| - |F_c||/\Sigma|F_o|$. $R_w = [\Sigma w||F_o| - |F_c||^2/\Sigma w|F_o|^2]^{1/2}$, $w = [\sigma^2(F_o) + \{0.015(F_o)\}^2]^{-1}$.

reflections. The intensities of three representative reflections measured after every 150 reflections remained constant throughout the data collection indicating the crystal stability. Empirical absorption corrections were made using the ψ-scan technique. The structures were solved by direct methods (SHELXS-86) [17], and successive difference Fourier syntheses were used to locate all non-hydrogen atoms. The structures were refined by full-matrix least-squares procedures. All non-hydrogen atoms were purified anisotropically, and hydrogen atoms were located at calculated positions with isotropic temperature factors equal to those for the attached atoms. Calculations were carried out using the Xtal 3.2 software [18].

Acknowledgements—The authors express their thanks to the Institute for Molecular Science, Okazaki, for allowing the use of facility of X-ray diffraction measurement. They also acknowledge Analytical Chemistry Laboratory, Faculty of Science, Nagoya University for the use of a Bruker AMX-400 NMR spectrometer.

REFERENCES

1. Trofimenko, S., *Chem. Rev.*, 1993, **93,** 943, and refs therein.
2. Buckingham, D. A. and Clark, C. R., *Comprehensive Coordination Chemistry*, p. 635, Vol. 4, G. Wilkinson, R. D. Gillard, and J. A. McCleverty, Eds; Pergamon Press: Oxford (1987).
3. Fujihara, T., Schönherr, T. and Kaizaki, S., *Inorg. Chim. Acta*, 1996, **249,** 135.
4. Curnow, O. J. and Nicholson, B. K., *J. Organomet. Chem.*, 1984, **267,** 257.
5. Jalón, F. A., Otero, A. and Rodríguez, *J. Chem. Soc. Dalton Trans.*, 1995, 1629.
6. Ventur, D., Wieghardt, K., Nuber, B. and Weiss, J., *Z. Anorg. Allg. Chem.*, 1987, **551,** 33.
7. Yoshikawa, Y. and Yamazaki, K., *Bull. Chem. Soc. Jpn.* 1972, **45,** 179.
8. Churchill, M. R., Gold, K. and Maw, C. E., Jr., *Inorg. Chem.*, 1970, **9,** 1597.
9. Thöm, V. J., Boeyens, J. C. A., McDougall, G. J. and Hancock, R. D., *J. Am. Chem. Soc.*, 1984, **106,** 3198.
10. Mikami, M., Kuroda, R., Konno, M. and Saito, Y., *Acta Cryst.*, 1977, **B33,** 1485.

11. Larsen, E., Larsen, S., Paulsen, G. B., Springborg, J. and Wang, D.-N., *Acta Chem. Scand.*, 1994, **48,** 107.
12. Kobayashi, M., Marumo, F. and Saito, Y., *Acta Cryst.*, 1972, **B28,** 470.
13. Konno, M., Marumo, F. and Saito, Y., *Acta Cryst.*, 1973, **B29,** 739.
14. Trofimenko, S., *Inorg. Synth.*, 1970, **12,** 99.
15. Crayton, P. H., *Inorg. Synth.*, 1963, **7,** 211.
16. Okamoto, M. S. and Barefield, E. K., *Inorg. Chim. Acta*, 1976, **17,** 91.
17. Sheldrick, G. M., SHELXS-86, Program for Crystal Structure Determination, University of Göttingen, Germany (1986).
18. Hall, S. R., Flack, H. D. and Stewart, J. M., Xtal 3.2, Program for X-Ray Crystal Structure Analysis. Universities of Western Australia, Geneva, and Maryland (1992).